The breakdown strength and localised structure of polystyrene as a function of nanosilica fill-fraction

M. Praeger, A.S. Vaughan, S.G. Swingler
Tony Davies High Voltage Laboratory
University of Southampton
Southampton, UK
mattp@soton.ac.uk

***Abstract*—In this work the amorphous matrix of polystyrene provides a homogenous basis into which nanosilica particles are added. Composites are made with four different types of nanosilica particles which are subsequently compared. The DC breakdown strength of the resulting nanocomposite materials is measured as a function of filler fraction with loadings between 0 and 10 %. One advantage of using a polystyrene matrix for this study is its compatibility with permanganic etching. This technique is used to remove part of the polystyrene matrix and render the configuration of the nanofiller particles within the composite amenable to examination by scanning electron microscope (SEM). The simple sample preparation protocol employed here resulted in significant nanofiller agglomeration and the DC breakdown strength was found to decrease with increasing filler fraction.**

Keywords—nano; silica; composite; polystyrene; dielectric; breakdown; permanganic; SEM

I. INTRODUCTION

The future development of electrical power networks and systems demands the creation of new high-performance dielectric materials. For example, highly rated HVDC cables are needed for the proposed transcontinental links of the European super-grid, where target ratings as high as 1 MV and 5 kA have been postulated. Enhancement of the basic properties of polymers with the addition of nanofillers is an attractive approach for achieving these high ratings and has been the subject of many studies [1, 2]. Perhaps the greatest potential for performance gains arises when nanofillers are employed as a tool to allow careful tailoring of material properties to the requirements of a specific application. Fabrication of such custom nano-dielectrics could, for example, allow cable designers to optimize insulation materials for compromises between thermal conductivity, operating temperature and DC breakdown strength [3].

Despite their potential benefits, fabrication of nanocomposites can be challenging; one area of particular difficulty is achieving uniform particle dispersal. Differing degrees of particle agglomeration are likely to be one of the main reasons for the considerable variability of results reported in the literature; however, particle agglomeration is neither readily measured nor regularly reported. Interpreting the literature is further complicated by the proliferation of different types of nanofillers.

The overarching aim of this work is to further our understanding of the mechanisms governing the action of nano-fillers. In this work we therefore use polystyrene as a simple matrix system for an investigation into the effect of silica nanofillers on electrical breakdown strength. Although polystyrene is not widely employed in power system applications, it does find practical uses as a dielectric in devices such as capacitors and has been reported to exhibit very high breakdown strength. However, its attraction in the context of this work is that it is an amorphous thermoplastic and, therefore, provides an ideal model system where factors such as variations in matrix morphology (c.f. polyethylene) or resin stoichiometric effects (c.f. epoxy resins) do not come into play. An additional benefit of polystyrene is that its chemistry is amenable to permanganic etching [4], which allows high resolution imaging techniques (SEM) to resolve the configuration of nanofillers in-situ within the nanocomposite system. Epoxy resins cannot be explored in this way, whilst in semicrystalline polyolefins the lamellar texture makes it difficult to determine the spatial distribution of the truly nanoscopic filler particles. The structure of the resulting nanocomposites is correlated with and discussed in relation to the measured breakdown strength.

II. METHOD

A. Sample Preparation

In this initial proof of principle study a very simple sample preparation procedure was followed. This procedure was not expected to yield optimal filler dispersal and in fact samples with some degree of particle agglomeration were required in order properly to test the permanganic etching technique. The basic steps of the sample preparation protocol are listed below:

- Weigh out nanosilica (NS) inside a glove box and add to dichloromethane (DCM).
- Sonicate the NS-DCM solution for 1 hour.
- Weigh out polystyrene (PS) and dissolve in DCM.
- Combine the sonicated NS-DCM and the PS-DCM solution by shaking for 1 hour.

The website for the Top & Tail Transformation project can be found at: http://www.topandtail.org.uk/

- Allow the DCM solvent to evaporate at room temperature for 3 days.
- Produce sample discs by pressing at 175 °C with 5 tons of pressure for 4 minutes.

The glove box is used (along with procedures such as triple bagging of nano-contaminated waste and a filtered external venting system) in order to prevent inhalation of the nanoparticles. A water bath sonicator is used to disperse the nanosilica within the DCM solution; to prevent overheating of the DCM the sonicator bath water is replaced at 15 minute intervals. If required, multiple pressings were used to remove residual solvent and gas bubbles from the samples.

B. DC Breakdown Measurements

DC breakdown measurements are made using a purpose built apparatus (see Fig. 1) which is operated within an interlocked metal cage. The disc shaped samples are held between two 6.35 mm diameter, chrome-plated, steel ball-bearings, the entire assembly is then immersed in silicone oil and a steadily increasing voltage (100 V/s) is applied between the ball-bearings. The silicone oil ensures that the path taken by the breakdown is through, rather than around, the test sample. A digital multimeter records the voltage applied between the ball-bearings immediately prior to DC breakdown of the test sample.

For each composition, 8 discs of approximately 75 µm thickness and 30 mm diameter were pressed. It was usually possible to obtain 4 breakdown measurements per disc. This DC breakdown data was studied using Weibull analysis [5].

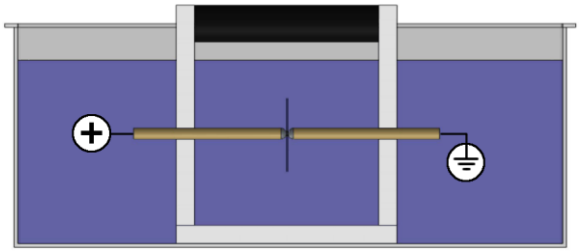

Fig. 1. A cut-away diagram of the DC breakdown apparatus. There is an integrated handle to lift the entire assembly out of the plastic tank of silicone oil and one of the rods is spring loaded to allow easy sample changes.

C. Permanganic Etching and SEM Imaging

Permanganic etching has been demonstrated to be a highly effective means of studying the structure of polymer materials. The technique relies on amorphous and crystalline regions of a material experiencing differing etching rates. It is thought that the etching solution penetrates the amorphous regions more readily and that this results in accelerated etching. In this way permanganic etching is capable of revealing crystalline structures, such as lamella or spherulites, within semi crystalline materials. Crystalline structures that were previously concealed are given increased relief; this makes SEM imaging possible and/or offers dramatically improved contrast.

In this work permanganic etching is used to remove a thin layer of the amorphous polystyrene matrix; the etchant is expected to have little effect on the silica nano fillers. The etching process therefore reveals the condition of the nanofillers in-situ within the nanocomposite material.

The permanganic etching procedure consists of the following key steps:

- The etchant mixture is produced; 5:2:1 of sulphuric acid, phosphoric acid and water.
- 1 % by weight of potassium permanganate is gradually added to the etchant mixture.
- The mixture is continuously stirred with no additional heating for 10-20 minutes. The mixture should turn dark green in colour.
- The samples are submerged in the etchant mixture and shaken throughout the desired etching duration.
- After etching the mixture is "quenched" by a 2:7 mixture of sulphuric acid and water to which 20% by volume of hydrogen peroxide is added.
- The samples are rinsed in distilled water and then in methanol.

Care must be taken when producing the etch and quench mixtures because significant heat is generated. Particular caution is required when adding the potassium permanganate as inadequate stirring could result in production of manganese heptoxide which is explosive.

III. RESULTS

A. DC Breakdown Strength vs Filler Type

Nanocomposite samples were produced using four different types of nanosilica filler (all supplied by Sigma Aldrich) according to the procedure described in Section II A. Details of the nanofillers used are provided in Table I. In each case the samples were given a nanofiller loading of 2.5 % by weight. Throughout the rest of this paper the nanofillers and their resulting nanocomposites will be referred to by the "Nano-filler type" labels denoted in Table I.

The DC breakdown results (see Fig. 2) appear to fall into two categories: The two nanocomposites produced from

TABLE I. NANOSILICA FILLER TYPES

Nano-filler type	**Supplier Data**		
	Description	***Supplier #***	***Particle size***
M	Silicon Dioxide, nanopowder (spherical, porous)	637246	5-15 nm
Q	Silicon Dioxide, nanopowder.	637238	10-20 nm
S1	Fumed silica powder (aggregate) Avg. part. Size 100-200 nm.	S5130	7 nm
S2	Fumed silica powder (aggregate) Avg. part. Size 200-300 nm.	S5505	14 nm

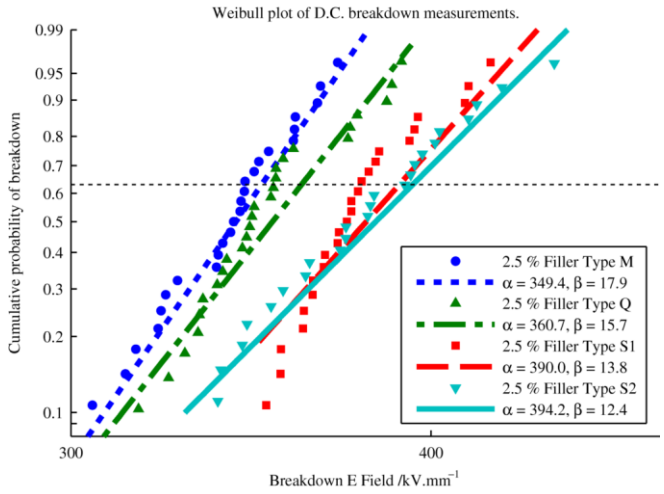

Fig. 2. Measured DC breakdown strength against filler type in polystyrene nanosilica composites with 2.5 % filler by weight.

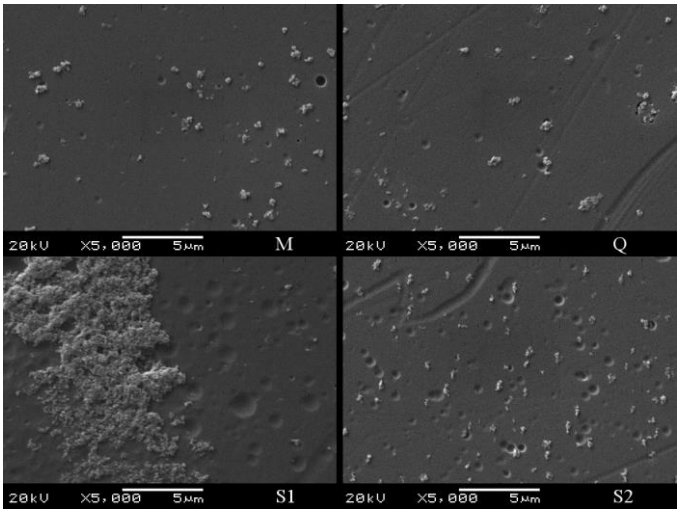

Fig. 3. SEM images comparing polystyrene nano composites with 2.5 % loading of four different filler types. The labels denote the filler type as shown in Table I. The 1 hour etched samples are shown except for the case of S1 where the 4 hour etched image is used because this clearly illustrates the non-uniformity of the particle distribution.

fumed silica powders (filler types S1 & S2) display very similar performance. These nanocomposites had breakdown strengths of 390 and 395 ±10 kV.mm^{-1} respectively. These two results are equivalent within experimental errors; furthermore, they show essentially the same breakdown strength as unfilled polystyrene samples (see Section III C). The nanocomposites made from filler types M and Q exhibit lower breakdown strength (349 and 360 ±10 kV.mm^{-1} respectively) but the steeper gradient of the Weibull fit and the larger β parameters indicate that the measured breakdown values were slightly more consistent (the 95 % confidence bounds for β are ±4).

B. Permanganic Etching and SEM vs Filler Type

The permanganic etching procedure described in Section II C was followed. Etch durations of 1, 2 and 4 hours were used in order to observe the etch progress as a function of time. After etching, the samples were mounted on pin stubs and gold coated to prevent surface charge accumulation during SEM imaging; the resulting images are shown in Fig. 3.

All of the samples contain particles that are larger than the dimensions given in Table I. At high magnification the granular structure of the particles is visible, confirming that these particles are agglomerations of primary units.

Just as with the DC breakdown data the SEM images also fall into two categories: For the M and Q type samples the agglomerated filler formed particles with typical diameters of approximately 500 nm. The distribution of particles throughout the M and Q type samples was fairly homogenous. In contrast, the particle distribution in the type S1 and S2 samples was patchy. Large regions of very high particle density were observed, whilst other areas were almost devoid of filler (see Fig. 3, S1). In regions where the particle density was similar to those observed for the M and Q type samples, the typical particle size was slightly lower at ~350 nm, (see Fig. 3, S2). For the M and Q type fillers the typical particle sizes were observed to increase as a function of etch duration;the same effect was not evident for the type S1 and S2 samples.

C. DC Breakdown Strength vs Filler Fraction

Nanocomposite samples were produced using filler type M and with filler fractions in the range 0 - 10 %; the DC breakdown results are shown in Fig. 4. In the Weibull analysis the fit lines run almost parallel; this indicates that the spread of DC breakdown values is very similar for each composition. The average β value for the Weibull fits is 10.7 with 95 % confidence bounds of ±3; this is lower than was achieved in the"filler type" measurements shown in Fig 2. These two data sets are derived from different batches of samples and so this discrepancy may be attributed to production variability.

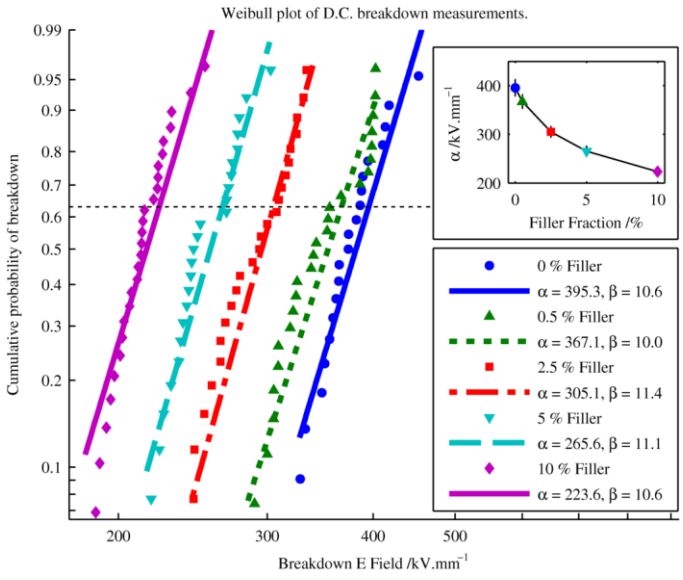

Fig. 4. Weibull analysis of DC breakdown measurements for polystyrene nanosilica composites with different nanofiller loadings. The inset in the upper right shows the DC breakdown strength as a function of filler fraction.

In Fig. 4 the intercept between the Weibull fits and the 62.3 % probability line moves steadily towards lower breakdown electric field as the filler fraction is increased. These breakdown strength data are plotted in the inset on the upper right of Fig. 4 which includes error bars that show the 95 % confidence bounds derived from the Weibull fit.

D. Permanganic Etching and SEM vs Filler Fraction

Once again the etching procedure described in Section II C was followed. Samples were prepared using different loadings of filler type M; SEM images of these samples are shown in Fig. 5. For obvious reasons there is a clear correlation between the filler loading and the spatial density of the particles. More interestingly, the typical particle size seems to be almost independent of the filler concentration. As noted in Section III B; the typical particle size for type M samples varies considerably more as a function of the etch duration. The samples shown in Fig. 5 were all etched for 2 hours except for the 2.5 % sample in Fig. 5C. This sample was processed in a different batch and appears to have experienced a higher etch rate; the 1 hour etched sample is therefore more comparable.

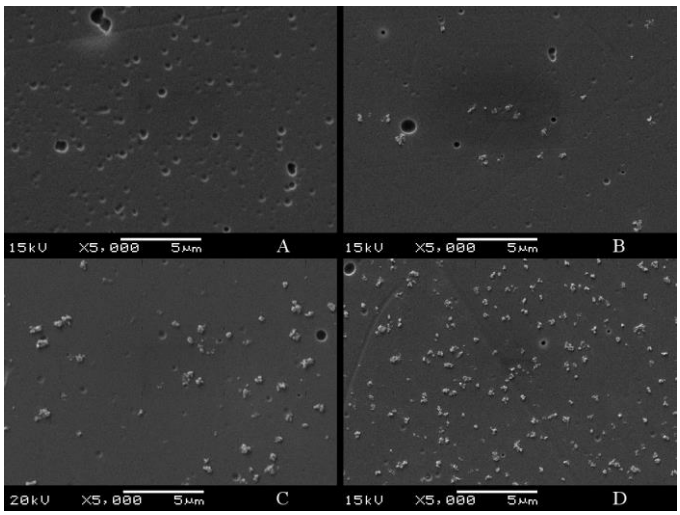

Fig. 5. SEM images of type M nano composites after permanganic etching. Images A to D show filler fractions of 0, 1, 2.5 and 10 % respectively.

IV. Conclusion

The DC breakdown data in Fig. 4 clearly show that as the concentration of nanofiller is increased the breakdown strength of the resulting nanocomposite is reduced. These data were obtained for the type M filler for which the particles, although agglomerated, were homogeneously distributed. The SEM images in Fig. 5 show that the agglomeration size is approximately independent of the filler concentration. The effect of filler concentration on the breakdown strength is therefore thought to be chiefly a result of the spatial density of the agglomerated particles. The agglomeration size is probably determined primarily by the sample preparation procedure; for example by the effectiveness and duration of sonication.

The Weibull analysis of the different filler types (Fig. 2) shows increased variability for filler types S1 and S2; probably due to the patchy filler dispersion. However, the highest breakdown values for the S1 and S2 samples were in line with those of the unfilled polystyrene (see Fig. 4) whilst the type M and Q fillers seem to degrade the performance. Conventional wisdom is that agglomerated regions dominate, and will decrease the DC breakdown strength; this is not the case here. An alternative explanation is that when the clusters are large enough (hundreds of microns in size but are distributed over mm scales) the dominant effect is an apparent reduction in filler density elsewhere in the sample. In this case breakdown measurements will be made most frequently in regions of low filler density and in accordance with Fig. 4 this would cause proportionally less reduction to the DC breakdown strength.

As supplied, the nanoparticles in fumed silica fillers S1 & S2 are fused together into chains several hundred nanometers in length. For the M and Q type samples the observed increase in particle size after 4 hours of etching may indicate that some of the filler has been released from the matrix and has begun to aggregate on the surface despite the shaking and rinsing procedures used. Consequently the 1 and 2 hour etched SEM images are most representative of the condition of the nanofiller "in-situ" within the nanocomposite. The fused particle chains in the type S1 and S2 samples may also hinder release of the filler particles from the matrix; this could explain why particle size did not increase with etch duration for these samples. Furthermore, the larger, fused particle chains in the S1 and S2 filler types may have reduced the effectiveness of sonication during sample preparation; this could therefore be responsible for the patchy dispersal of filler in these samples.

Permanganic etching and SEM imaging have been demonstrated as an effective technique for studying the condition of nanofillers "in-situ" within an amorphous polymer nanocomposite. This information helps us to understand what happens to the nanofillers during sample preparation and informs new protocols. Correlating the filler condition with measured properties of the nanocomposite (such as breakdown strength) reveals which aspects of the filler distribution are critical for control over these properties. This information is vital when customizing nanodielectrics to specific applications.

Acknowledgment

The authors gratefully acknowledge the RCUK's Energy Programme for the financial support of this work through the Top & Tail Transformation programme grant, EP/I031707/1.

References

[1] Y. Cao, P. C. Irwin, and K. Younsi, "The Future of Nanodielectrics in the Electrical Power Industry," *IEEE Trans. Diel. Electr. Insul.*, vol. 11, pp. 797-807, Oct 2004.

[2] T. J. Lewis, "Nanometric Dielectrics," *Ieee Trans. Diel. Electr. Insul.*, vol. 1, pp. 812-825, Oct 1994.

[3] J. A. Pilgrim, P. L. Lewin, and A. S. Vaughan, "Quantifying the Operational Benefits of new HV Cable Systems in Terms of Dielectric Design Parameters," *2012 IEEE Int. Symp. Electr. Insul. (ISEI)*, pp. 261-265, 2012.

[4] R. H. Olley, A. M. Hodge, and D. C. Bassett, "Permanganic Etchant for Polyolefins," *Journal of Polymer Sci.: Part B-Polym. Phys.*, vol. 17, pp. 627-643, 1979.

[5] L. A. Dissado, J. C. Fothergill, S. V. Wolfe, and R. M. Hill, "Weibull Statistics in Dielectric-Breakdown - Theoretical Basis, Applications and Implications," *IEEE Trans. Electr. Insul*, vol. 19, pp. 227-233, 1984.